Giant monopole resonance in Sn and Sm nuclei and the compressibility of nuclear matter

M. M. Sharma
Kernfysisch Versneller Instituut, 9747 AA Groningen, The Netherlands
and Sektion Physik, Universität München, D-8046 Garching, Federal Republic of Germany

W. T. A. Borghols, S. Brandenburg, S. Crona, and A. van der Woude
Kernfysisch Versneller Instituut, 9747 AA Groningen, The Netherlands

M. N. Harakeh
Natuurkundig Laboratorium, Vrije Universiteit, 1007 MC Amsterdam, The Netherlands
(Received 6 January 1988; revised manuscript received 25 July 1988)

A study of the systematics of the breathing mode giant monopole resonance in the isotopic chains of Sn and Sm nuclei by means of inelastic scattering of 120 MeV alpha particles at 0° has been performed. The obtained energy systematics for spherical Sn and Sm nuclei have been employed to fit the nuclear-compressibility parameters. The data on Sn and Sm nuclei have been used in conjunction with already existing data on ^{208}Pb and ^{24}Mg to constrain the various parameters contributing to the nuclear compressibility. The compressibility of nuclear matter K_∞ has been deduced to be 300±25 MeV, in contrast with the commonly accepted value of 210±30 MeV. The neutron-asymmetry term has been determined to be −320±180 MeV.

I. INTRODUCTION

The isoscalar giant monopole resonance (GMR), the so-called breathing mode, is of particular interest due to its bearing with the compressibility of nuclei and hence to the compressibility of nuclear matter. The hydrodynamical model relates in a simple way the compressibility of a nucleus to the frequency of vibration of the GMR as

$$E_0=\hbar\omega_0=\hbar[K_A/(m\langle r_0^2\rangle)]^{1/2}\ , \tag{1}$$

where m is the nucleon mass and $\langle r_0^2\rangle$ is the rms radius of the nucleus. The incompressibility (many times referred to as compressibility) K_A of a nucleus of mass A is defined by

$$K_A=R^2\frac{d^2(E/A)}{dR^2}\bigg|_{R=R_0};\quad R=\langle r_0^2\rangle^{1/2}\ . \tag{2}$$

Using the semiempirical mass formula[1] and taking the second derivative of E/A, one obtains the expression for K_A as

$$K_A=K_\infty+K_S A^{-1/3}+K_\tau\left[\frac{N-Z}{A}\right]^2+K_C Z^2 A^{-4/3}\ , \tag{3}$$

where K_∞, K_S, K_τ, and K_C are the second derivatives of coefficients of volume, surface, neutron-excess, and Coulomb terms, respectively, in the mass formula with respect to the radial coordinate of the nucleus as in Eq. (2). The Coulomb term, K_C, can be obtained analytically[2] assuming a uniform density for the nucleus within a sphere of radius R_C:

$$K_C=\frac{6e^2}{5r_C}\ . \tag{4}$$

Blaizot[3] has shown that by properly taking into account the equilibrium condition of the nuclear ground state, one obtains a different relation

$$K_A=K_\infty+K_S' A^{-1/3}+K_\Sigma'\left[\frac{N-Z}{A}\right]^2+K_C' Z^2 A^{-4/3}\ , \tag{5}$$

where K_C' is different from the one in Eq. (3) as will be discussed in the section below and where the coefficients K_S', K_Σ', and K_C' do not have the simple interpretation of being the second derivatives of the respective terms in the mass formula. In Eq. (5) the coefficients K_∞, K_S', and K_Σ' are related to K_A as given by expression 6.3 of Ref. 3. Also there exists a dynamical coupling between the surface and bulk vibrations as pointed out by Brack and Stocker.[4] The parameter of prime interest in Eq. (5) is K_∞, the compressibility of infinite nuclear matter. This is usually determined by a three-parameter fit to the experimental GMR energies according to Eqs. (1) and (5). It has been shown by Treiner *et al.*[5] that in the scaling model of the breathing mode vibration, which we assume throughout this paper, the $A^{-1/3}$ expansion of K_A [see, for example, Eq. (5)] converges rapidly. For light nuclei, however, addition of a curvature term (which goes as $A^{-2/3}$) becomes necessary in Eq. (5) as pointed out by these authors.[5] The associated coefficient $K_{\rm curv}$ has been estimated to be about 300 MeV (Ref. 5).

The present work has been performed with the aim to improve the precision with which the various parameters in Eq. (5) can be determined from the data on the nuclear compressibilities K_A by obtaining more accurate data on the GMR for Sn and Sm nuclei. This is especially impor-

tant for K_∞ which is required in the description of supernova explosions.[6]

II. PRESENT STATUS ON COMPRESSIBILITIES

The experimental data on the isoscalar GMR for a large number of nuclei have been used to fit Eq. (5) to obtain the values of various coefficients contributing to K_A (Refs. 7–16). However, these parameters still have large uncertainties associated with them. This is especially true for K'_Σ which has been deduced with large uncertainties and with values between -250 and -600 MeV. The surface parameter K'_s obtained varied between -400 and -700 MeV while the values of K_∞ lie between 200 and 300 MeV. Thus, by using these data the compressional modulus of nuclear matter is rather poorly known. As the light nuclei show a predominant surface effect, their inclusion in the experimental systematics towards the search for nuclear compressibility is important. Only recently has the experimental situation on the GMR in light nuclei been clarified, thus making a more precise determination of K_∞ possible.[12,13]

On the theoretical side, Blaizot *et al.*[14,15] have performed self-consistent RPA calculations on ^{16}O, ^{40}Ca, ^{90}Zr, and ^{208}Pb nuclei using various Skyrme interactions. The obtained values of K_A were fitted to Eq. (5) to determine various coefficients. The value of K'_s obtained from such fits was between -350 and -500 MeV and the value of K'_Σ was found between -400 and -500 MeV. The nuclear-matter compressibility K_∞ thus obtained lies between 260 and 350 MeV depending on the effective interaction used in the calculations. Furthermore, in a comparison of ^{208}Pb calculations with the experimentally known results, Blaizot[3] has determined $K_\infty = 210 \pm 30$ MeV which is presently the "commonly accepted" value. However, this value is based upon comparison of the calculations for only one nucleus (^{208}Pb) with experiments. For a proper comparison of experimental results with theory, the RPA calculations are required for a number of nuclei including light to heavy.

Microscopic calculations for the nuclear-matter compressibility have resulted in varying conclusions. Using Landau-Fermi liquid theory, Brown and Osnes[17] determined the compression modulus to be $K_\infty \leq 106$ MeV. This result shows a consistency with the works of Dickhoff *et al.*[18] and Jackson *et al.*[19] who obtained K_∞ below 100 MeV. All these calculations are in conflict with the experimental results obtained so far, which indicate values of K_∞ of approximately 200 MeV. In a relativistic Dirac-Brueckner approach ter Haar and Malfliet[20] have obtained an equation of state for nuclear matter with compressibility $K_\infty \sim 250$ MeV. This value is within reasonable agreement with the experimental values of K_∞. Recently Ainsworth *et al.*[21] have modified the previous results of Ref. 17 and have obtained an equation of state for dense nuclear-matter with $K_\infty \approx 180$ MeV. This is apparently close to K_∞ required in supernova explosions in the work of Ref. 6.

Có and Speth[22] have tried to determine the nuclear-matter compressibility by analyzing the charge-density difference between ^{208}Pb and ^{207}Pb and between ^{208}Pb and ^{206}Pb obtained from elastic electron scattering. They have pointed out that the polarization of the density distribution which is sensitive to the interior of the nucleus, can be used as a measure of the nuclear-matter compressibility. The analysis shows that the experimental charge-density difference is compatible with a value of K_∞ of approximately 345 MeV. The values at about and below 200 MeV seem to be excluded according to these authors. It has been pointed out by Bartel *et al.*[23] that Có and Speth[22] did not include the pairing effect, which makes the analysis of the ^{208}Pb-^{206}Pb charge-density difference doubtful. Incidentally, Cavedon *et al.*[24] have been able to reproduce the experimental charge-density difference between ^{207}Pb and ^{208}Pb in a mean-field calculation using the density-dependent force $D1$ of Gogny with a compressibility $K_\infty = 230$ MeV with an uncertainty of ± 30 MeV.

III. EXPERIMENTAL SITUATION ON THE GIANT MONOPOLE RESONANCE

The existence of the giant monopole resonance (GMR) in medium and heavy nuclei has been well established.[7–11] The centroid energy of the broad GMR bump observed experimentally in hadronic inelastic scattering has been found to be quite close to the prediction $E_x = 80 A^{-1/3}$ MeV of the hydrodynamical model. Most of the data on the GMR have been obtained with alpha particle or ^{3}He beams. The obtained results have been widely used to fit the parameters K_∞, K'_s, and K'_Σ, as mentioned above.

For nuclei with $A < 120$, the centroid energies of the GMR deviate increasingly from the hydrodynamical prediction indicating the importance of surface effects. The width of the GMR has been found to decrease from 4 to 2.5 MeV as the mass increases from 100 to 200 except in the deformed nuclei. Furthermore, in light nuclei, for instance, ^{24}Mg (Ref. 12) and ^{28}Si (Ref. 13), the GMR is observed to be fragmented over a wide excitation energy interval; the same being true for the giant quadrupole (GQR) and the giant dipole resonances (GDR) (Ref. 11). Until a few years ago, it was believed that the GMR does not exist in light nuclei. At that time the data indicated that the strength of the GMR decreased from about 100% EWSR in heavy nuclei ($A > 150$) to 10–30% in light nuclei. However, recently up to 90% of the $E0$ EWSR has been observed in the GMR of ^{24}Mg (Ref. 12) and 65% in ^{28}Si (Ref. 13). This makes it possible to include these data in the fit for K_∞.

IV. AIM OF THE PRESENT EXPERIMENT

As mentioned before, the nuclear-matter compressibility K_∞ and the associated coefficients K'_s and K'_Σ are not yet known very accurately. In order to determine these parameters with better accuracy, we have performed inelastic scattering of 120 MeV alpha particles at very small angles including 0° on the isotopic chains of Sn and Sm nuclei. In an isotopic chain the contribution to K_A [Eq. (5)] arises from various terms, predominantly from the surface term designated as $A^{-1/3}$ and the asymmetry

term. The Coulomb term varies only by a small amount. Because of the strong correlation between various parameters in Eq. (5), a better determination of these parameters will result in a better determination of K_∞.

Previous experiments on the Sn and Sm isotopes (Refs. 7 and 8), as summarized in Ref. 8, gave values for the centroid energy with uncertainties varying from 250 to 600 keV. These uncertainties stem from the presence of a different experimental background and from different shapes and magnitudes of the nuclear continuum generated by the inelastic scattering of different probes. The analysis requires an accurate decomposition of the experimental spectrum into the resonance and the background, the latter consisting of the instrumental and continuum types. Since the continuum in heavy nuclei is large compared to the contents of the resonances, and furthermore, since the GMR and GQR bumps overlap each other, the determination of the systematics of the GMR entails the decomposition of the broad bump into the GMR and GQR contributions besides selecting a proper underlying background. This procedure is likely to be associated with large uncertainties.

In our analysis, the instrumental background is removed by setting software gates on various parameters delivered by the two-dimensional position sensitive detection (psd) system such as vertical and horizontal angles of incidence, time of flight of the α particles and energy deposited in the scintillator. Furthermore, in our analysis we have employed a method-of-difference spectrum,[25] which we will discuss below. The method results in a final spectrum in which the continuum background as well as the GOR component are reduced substantially. This leads to a large reduction in the uncertainties associated with the systematics of the GMR in our experiment and thereby increases the reliability of the compressibility parameters obtained.

V. EXPERIMENTAL DETAILS

The inelastic α-scattering was performed at 120 MeV incident energy. The 120 MeV analyzed beam was obtained from the AVF cyclotron at KVI Groningen. The targets were self-supporting with thicknesses between 0.75 to 1.5 mg/cm^2 and isotopically enriched to 99%. The use of the QMG/2 magnetic spectrograph[26] enabled the separation of the inelastically scattered α-particles at 0° from the outgoing beam. The spectrograph was set at 0°, with a full horizontal opening angle of $\Delta\theta=6°$ ($-3°$ to $+3°$) and a vertical opening angle of $\Delta\phi=4°$ ($-2°$ to $+2°$). The 52 cm long two-dimensional position-sensitive detection (psd) system[27] at the focal plane of the spectrograph was used to detect the inelastically scattered α particles. The beam was stopped in a graphite Faraday cup which was shielded from the detector system by a 10 cm thick lead wall. The angular resolution of the detector system was $\Delta\theta=0.7°$. The excitation energy range of 10–20 MeV, which encompasses the GMR and the GQR in these nuclei was covered.

The beam was analyzed with a double-focusing analyzing magnet in which the entrance and the divergence slits were set to limit divergence of the beam to 2 mm mrad in both the vertical and horizontal directions. Most of the beam halo due to slit scattering, etc. was minimized by adjusting the slit settings in the beam-transport system prior to the beginning of the experiment. The remaining beam halo was eliminated to a large extent by the time-of-flight of the particle with respect to the cyclotron RF, and plotted against the excitation energy, the details of which are given in Ref. 25.

VI. DATA ANALYSIS

The angular distribution of the $E0$ (GMR) and the $E2$ (GQR) calculated using the distorted wave-Born approximation (DWBA) for ^{112}Sn exhausting the full energy-weighted sum-rule (EWSR) are shown in Fig. 1. In the angular range (0°–3°) covered in our experiment, the isoscalar GMR has the steepest angular distribution, which drops by about two orders of magnitude going from 0° to 3°. On the other hand, the GQR which is the only other predominant mode of isoscalar collective excitation in the energy range covered in this experiment, has an almost flat angular distribution in this angular range. The same holds for higher multipole strengths. The situation for all Sn nuclei and Sm nuclei is similar to this representative picture in Fig. 1. In the analysis of the data, the whole angular range (0°–3°) software was divided into two bins, $0°<\theta<1.5°$ and $1.5°<\theta<3°$. The excitation energy spectra corresponding to these two bins were obtained after subtracting most of the instrumental background.

Figure 2 shows the excitation energy spectra of ^{112}Sn using the method discussed above. The resonance bump

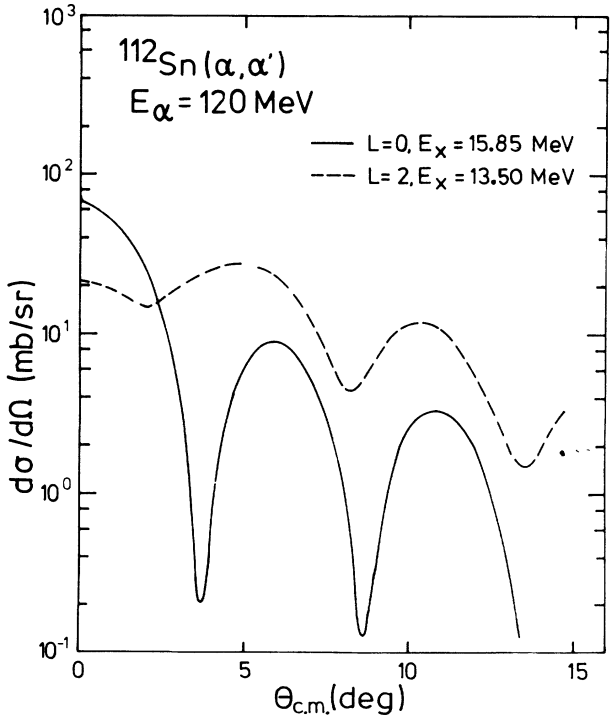

FIG. 1. The differential cross section of the GMR ($L=0$) and the GQR ($L=2$) calculated in DWBA for the respective full EWSR being exhausted in ^{112}Sn.

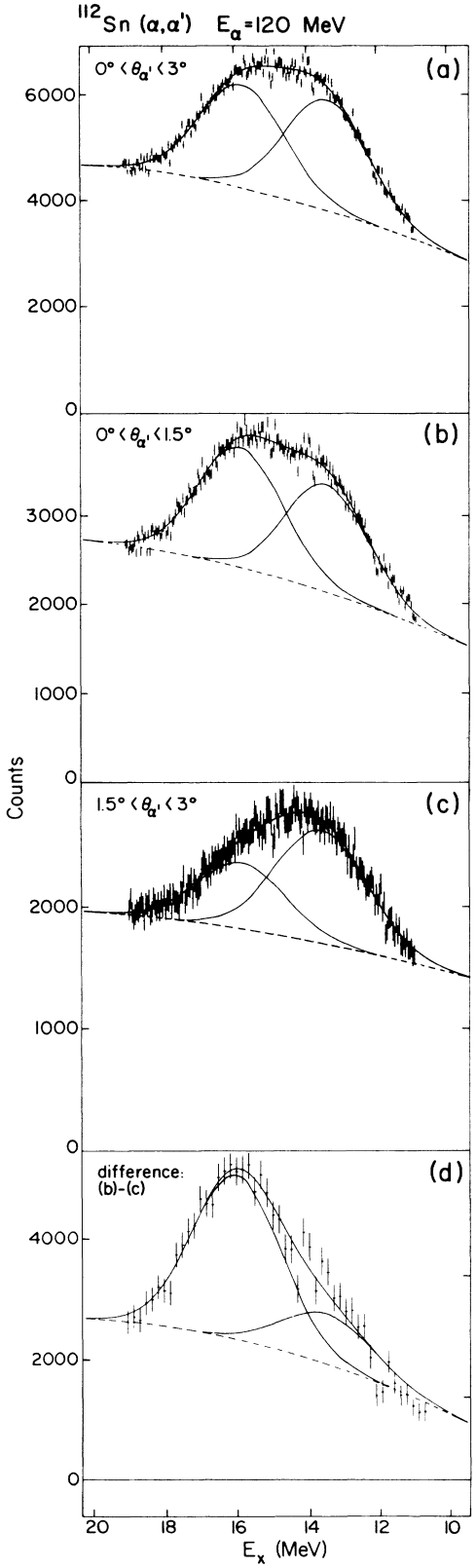

in all spectra was fitted to two Gaussians corresponding to the GMR and GQR by the method of least squares and minimization of χ^2. Figure 2(a) shows the excitation energy spectrum for the full angular range (0°–3°) depicting a significantly populated GQR on the lower energy side (with a centroid at ~13.5 MeV) and the GMR on the higher energy side (peaking at ~15.5 MeV) on top of a continuum background indicated by a dashed curve. A similar spectrum obtained for the first half of the angular bin (0°–1.5°) is shown in Fig. 2(b). The contribution of the GMR is seen to be dominant over the GQR as predicted by the DWBA calculations shown in Fig. 1. Figure 2(c) displays the corresponding spectrum for the lateral angles (1.5°–3.0°) where only a small GMR component is visible, evidently due to a very steep fall of the GMR angular distribution in this angular range. As the GQR angular distribution is more or less flat in the full angular range covered, the spectrum in Fig. 2(d) has been obtained by subtracting the spectrum due to lateral angles (c) from that due to small angles (b). The resulting spectrum carries only a very small part of the GQR strength as compared with a major contribution from the GMR. The parameters of the GMR have been obtained from this spectrum in which not only the GQR contribution is reduced, but also a small residual amount of the underlying continuum (shown by dashed curves in all spectra) resulting in a much better peak to continuum ratio for the GMR. Consequently, the method leads to a better determination of the systematics of the resonance under consideration.

As the continuum background is not well defined in giant resonance experiments, this usually increases the uncertainty in determining the resonance parameters. In our data analysis a constraint was provided on the shape of the background in all spectra (a) to (d) by fitting them in a consistent manner with respect to each other. In this procedure, the background of spectrum (c) is within the uncertainties the difference of the backgrounds in (a) and (b); and, similarly, the background of the final spectrum (d) is also roughly the difference between the backgrounds of spectra (b) and (c), while maintaining a consistent set of parameters for the GMR and the GQR from fits of all four spectra (a) to (d). Also, a little change in the shape of the continuum does not appreciably affect the GMR parameters. Ultimately, the ratios of the intensity of the GMR and the GQR for the two angular bins extracted from Figs. 2(b) and 2(c) are compared with the ratios of the cross sections calculated in the DWBA and averaged over the opening angle of the detector. The whole procedure of fitting the spectra and selecting the background as discussed in this section has been applied to all Sn and Sm isotopes. The experimental ratios thus obtained are compared with DWBA predictions in Table I. It can be seen that the experimental intensity ratios of the GQR for all Sn and Sm nuclei are in fair agreement with the

FIG. 2. The excitation energy spectra for ^{112}Sn(α,α'). Parts (a), (b), and (c) show the excitation energy spectra for the full angle (0°–3°), the small angle (0°–1.5°), and the lateral angle (1.5°–3°) bins, respectively. The spectrum (d) denotes the difference between the spectra of the small angle and the lateral angle bins. Each spectrum has been fitted to two Gaussians corresponding to the GMR (higher energy) and the GQR (lower energy) bumps shown by solid curves. The continuum background underlying the spectra is shown by dashed curves. The spectrum (d) has been squeezed by a factor of 4 as compared to the other spectra.

TABLE I. The ratio of the intensity of the GMR and of the GQR in the two angular bins (0°–1.5°) and (1.5°–3°), after decomposition of the broad bump into the GMR and the GQR. The ratios obtained with the DWBA cross sections averaged over the opening angle of the detector are also shown for comparison.

	GMR		GQR	
Nucleus	Experiment	DWBA	Experiment	DWBA
^{112}Sn	2.29±0.27	3.41	1.18±0.15	1.05
^{114}Sn	2.17±0.38	3.46	1.22±0.21	1.05
^{116}Sn	2.42±0.41	3.52	1.26±0.24	1.05
^{120}Sn	2.22±0.31	3.63	1.08±0.16	1.04
^{124}Sn	2.18±0.30	3.75	1.16±0.17	1.04
^{144}Sm	2.65±0.22	3.97	1.14±0.14	1.04
^{148}Sm	2.65±0.37	4.09	1.26±0.27	1.03
^{150}Sm	2.96±1.8	4.15	1.43±0.48	1.03
^{152}Sm	2.54±0.9	4.18	1.22±0.28	1.02

DWBA estimates. On the other hand, the DWBA intensity ratios for the GMR seem to be larger than the experimentally determined ones. These depend sensitively, however, on two effects: first, the resolution with which the incident angle is determined and second, its uncertainty. For example, if we assume that the angular bins were in fact 0°–1.4° and 1.4°–3°, then the DWBA intensity ratios for the monopole decrease by about 20% whereas the effect is smaller for the GQR.

VII. RESULTS AND DISCUSSION

A. Sn nuclei

The systematics of the GMR and the GQR as obtained following the procedure discussed in Sec. VI are summarized in Tables II and III. The full-angle (0°–3°) spectra for all Sn nuclei are displayed in Fig. 3. Our full-angle spectra are similar to the excitation-energy spectra obtained in the other experiments summarized in Ref. 8, wherein, however, a larger continuum background was present. It may be noticed that the slope of the continuum in the region of the GQR as it results from our analysis decreases in going from ^{112}Sn to ^{124}Sn. This observation seems to be consistent with the fact that the neutron-emission threshold decreases from 11 MeV for ^{112}Sn to 8.5 MeV for ^{124}Sn, if it is assumed that an appreciable fraction of the background is due to neutron knockout which might well be the case in medium heavy nuclei such as these.

TABLE II. The GMR parameters obtained for Sn and Sm nuclei. The uncertainties in the energies are the total errors including the systematic errors.

Nucleus	E_x (MeV)	Γ (MeV)	EWSR (%)
^{112}Sn	15.88±0.14	3.30±0.25	106±24
^{114}Sn	15.80±0.14	3.52±0.29	107±23
^{116}Sn	15.69±0.16	3.73±0.39	101±22
^{120}Sn	15.52±0.15	3.92±0.35	94±20
^{124}Sn	15.35±0.16	3.40±0.35	108±22
^{144}Sm	15.13±0.14	3.34±0.21	125±26
^{148}Sm	14.95±0.14	3.22±0.29	117±27
^{150}Sm	14.97±0.18	2.86±0.50	99±35
^{152}Sm	15.56±0.18	3.13±0.52	86±25

TABLE III. The GQR parameters obtained for Sn and Sm nuclei. The uncertainties in the energies are the total errors including the systematic errors.

Nucleus	E_x (MeV)	Γ (MeV)	EWSR (%)
^{112}Sn	13.51±0.13	3.15±0.23	123±26
^{114}Sn	13.53±0.14	3.03±0.26	140±35
^{116}Sn	13.39±0.14	2.94±0.31	134±28
^{120}Sn	13.24±0.13	2.88±0.20	135±27
^{124}Sn	13.02±0.13	2.80±0.30	127±31
^{144}Sm	12.70±0.14	2.62±0.20	123±29
^{148}Sm	12.66±0.15	2.60±0.30	87±27
^{150}Sm	12.75±0.17	2.85±0.36	132±50
^{152}Sm	12.78±0.17	3.63±0.42	183±50[a]

[a]Includes low-energy component of the GMR.

The systematics of the GMR, the mode which is of prime interest in this study are shown in Table II and the same are displayed in Fig. 6 (see further on). The centroid-energy variation of the GMR is rather smooth as shown by the big dots with error bars. It may be noticed that the error bars in the centroid energy are typically about 140–160 keV, which includes the statistical errors of 70–90 keV associated with the fits, the experimental uncertainties in the energy calibration, and the systematic errors due to the uncertainties in the shape of the underlying continuum. This holds for both Sn and Sm nuclei which were measured in the same experiments using the same experimental setup. These uncertainties are small compared to uncertainties of 200–400 keV in previous works on the GMR (Ref. 8). Also shown in Fig. 6(a) (by squares) are the energy systematics of the GMR for Sn nuclei from Grenoble data.[8] The dashed line joining these points where the errors in the energies are roughly ±250 keV (not shown in the figure) show a steeper slope than our data. The present results for the GMR for the Sn nuclei are also in good agreement with previous ^{116,118,120,124}Sn results,[7] taking into account the relative large uncertainties of 300–600 keV and 300–700 keV in the centroid energy and width respectively, as quoted in Ref. 7. It must be mentioned that the centroid energies for Sn nuclei follow a 76–77 $A^{-1/3}$ trend which is close to the hydrodynamical description. We will use these results later in the context of the compressibility calculations.

Another interesting point which is noteworthy is that the width of the GMR increases with mass from ^{112}Sn up to ^{120}Sn and seems to decrease for ^{124}Sn as shown in Fig. 6(b). A similar effect has recently been observed theoretically by Di Toro *et al.*[28] in a study of the effect of the ground state deformation on the width of the giant dipole resonance. The effect was attributed by these authors to be due to the position of the nucleus between two major

shells. Our results on the width of the GMR may possibly be explained by the same effect.

The transition strengths of the GMR and the GQR have been determined in terms of the deformation parameter β, which is obtained by comparing the experimental cross sections with the DWBA predictions as

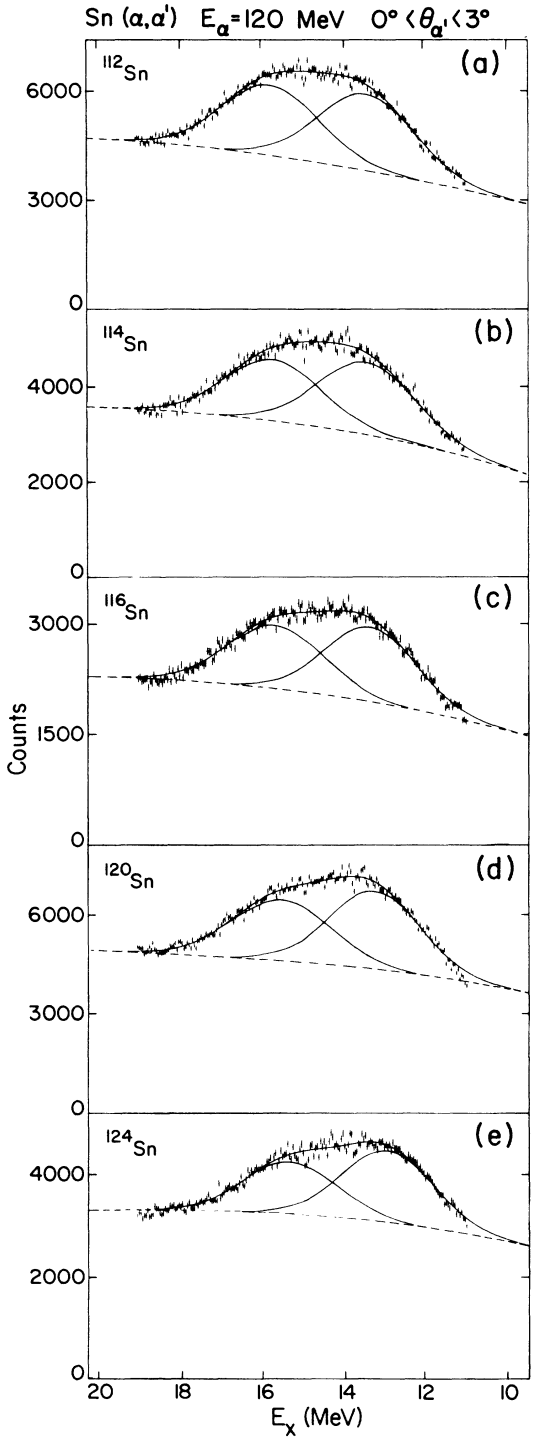

FIG. 3. The full-angle (0°–3°) spectra for Sn isotopes. Each spectrum shows the GMR and the GQR components and the underlying continuum background.

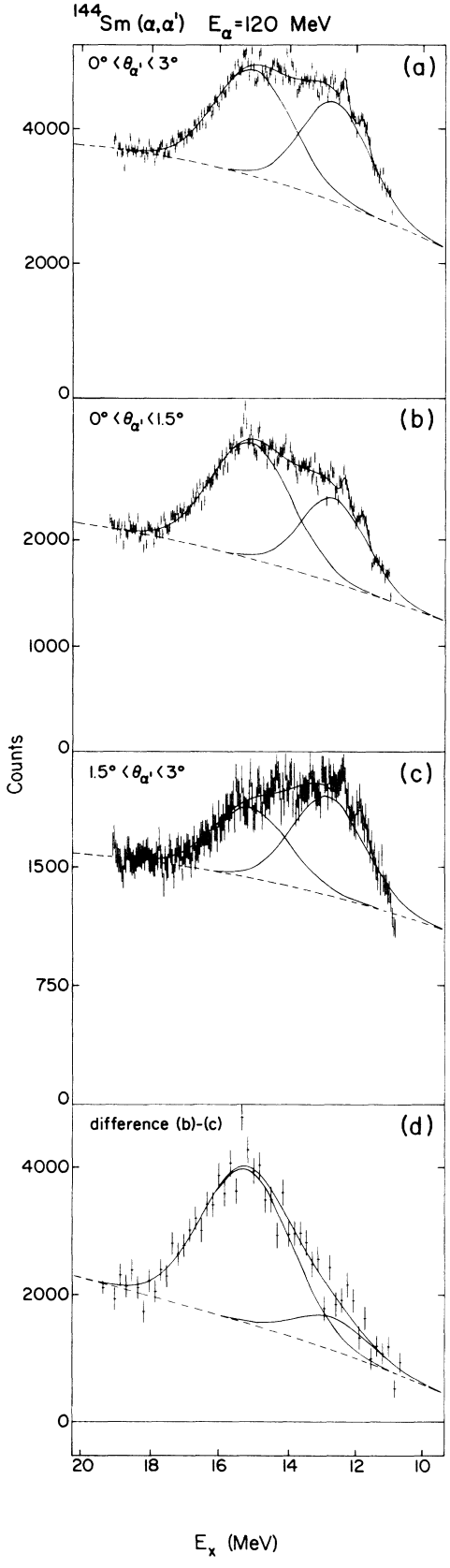

FIG. 4. The excitation energy spectra for ^{144}Sm(α,α'). The caption for this figure is similar to that of Fig. 2.

$$\beta^2 = \frac{d\sigma}{d\Omega}\bigg|_{\text{exp}} \Big/ \frac{d\sigma}{d\Omega}\bigg|_{\text{DWBA}} . \quad (6)$$

The prescription of Satchler (version I) (Ref. 29) for the transition density of the monopole breathing mode has been used to calculate the DWBA cross section. The form factor (transition density) for the GQR has been taken to be of the usual surface type. The optical potential parameters for the DWBA calculations were taken from Ref. 30. The deformation parameters β have been used to calculate the fraction of the EWSR exhausted in the reaction. The transition rates $B(E\lambda)$ were obtained from the radial moments of the real part of the optical potential as described in Refs. 31 and 32. The products $E_x\ B(E\lambda)$ were compared to the EWSR derived from a ground-state Fermi distribution to obtain the percentages of the EWSR exhausted by the GMR and GQR. The results are shown in Tables II and III. The uncertainties in the strengths are about 20–25% for both giant resonances. This uncertainty in the transition strength includes the uncertainty in the target-thickness measurement and the statistical errors associated with the fitting of the bumps. The GMR in all Sn nuclei seems to exhaust the full $E0$ sum rule, while for the GQR the data indicates a strength a little more than the full $E2$ sum rule. This is presumably due to the presence of the $L=4$ ($2\hbar\omega$) component at the position of the GQR (Ref. 11).

B. Sm nuclei

The samarium nuclei included in our study of the GMR are ^{144}Sm, ^{148}Sm, ^{150}Sm, and ^{152}Sm. The first three are known to be vibrational nuclei and are considered to be more or less spherical. On the other hand, the ^{152}Sm nucleus exhibits the properties of a deformed rotor in its ground state, with the ground-state deformation being $\beta=0.304$ (Ref. 33). It has been shown[34–37] that the GMR splits into two components due to the deformation of the nucleus. We also observe this effect in the case of ^{152}Sm, as we will discuss later. However, this is not the subject of the present study, and we include in the fit for the nuclear compressibility only ^{144}Sm and ^{148}Sm, for which there is no splitting of the GMR.

The spectra obtained for ^{144}Sm following the procedure as used in the case of Sn nuclei, are shown in Fig. 4. The spectra (a)–(d) in this figure are similar to those described for Sn nuclei in Sec. VII A. This is a representative figure for Sm nuclei and the spectra for all other Sm nuclei are similar to the ones for ^{144}Sm. The spectra have been fitted into two broad resonances above the nuclear continuum displayed by dashed curves. In addition to the GMR and the GQR, two narrow peaks at 11.52 MeV and 12.053 MeV are seen in parts (a), (b), and (c) of Fig. 4 which are due to inelastic scattering from ^{16}O present as a contaminant in the target. The ^{16}O peaks being narrow, were fitted by the least-squares method along with the broad resonances and thus do not influence the systematics. These peaks, moreover, proved to be useful in providing a redundant check of the energy calibration of the spectra.

The spectra for the full-angle (0°–3°) bin for samarium isotopes are shown in Fig. 5. As in Fig. 3 for Sn nuclei, the spectra for Sm isotopes also show a large continuum background underlying the resonance peaks. The oxygen

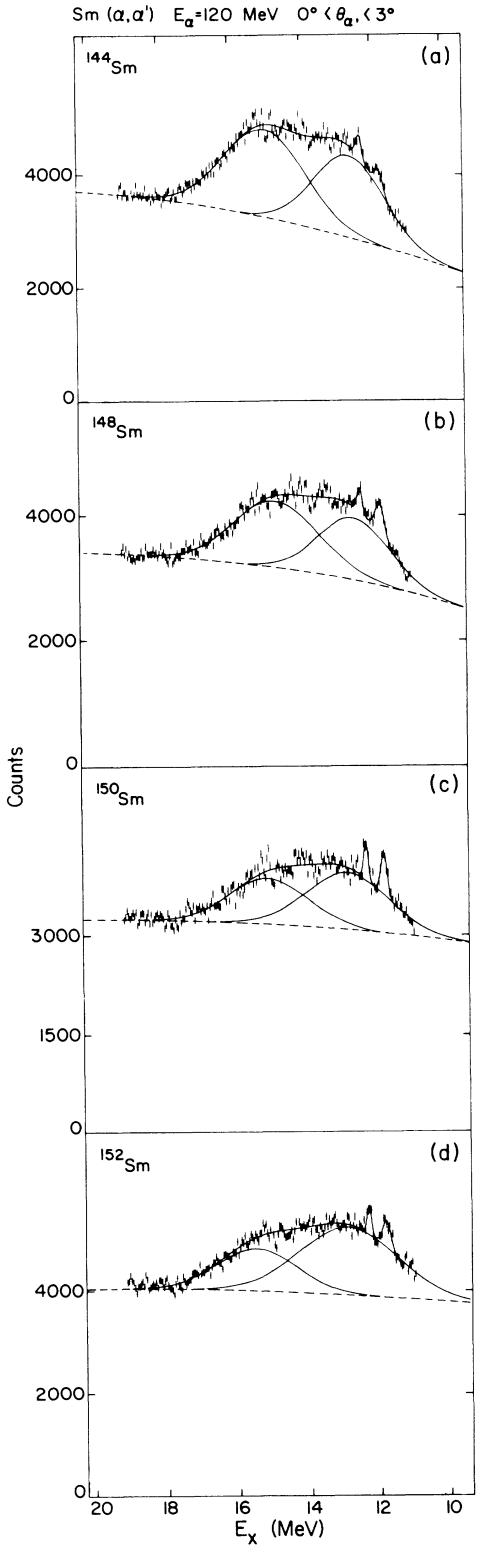

FIG. 5. The full-angle spectra for Sm isotopes showing the GMR, the GQR, and the continuum background. Two narrow contaminant peaks of oxygen on the lower energy side of the spectra are also observed.

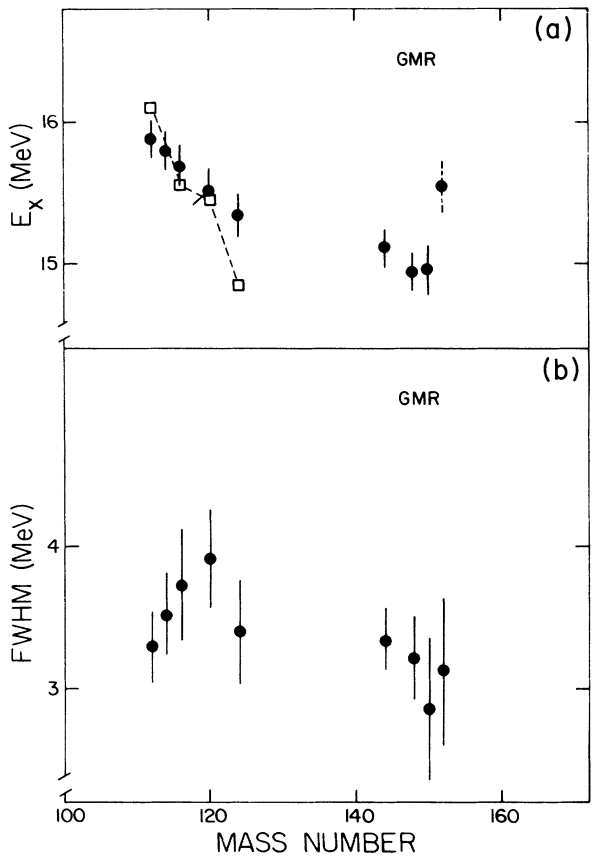

FIG. 6. The centroid energy and the width of the GMR peaks obtained from the fits for Sn and Sm isotopes. The data points for four Sn nuclei from Ref. 8 are also shown by empty squares. The centroid energy for ^{152}Sm which is deformed are shown by dashed error bars.

peaks are observed in all spectra and have been fitted in addition to the GMR and the GQR bumps. The systematics of the GMR and the GQR obtained from the fits for Sm nuclei are listed in Tables II and III. The results for the GMR are also displayed in Fig. 6. The centroid energy and width of the GMR for ^{144}Sm, ^{148}Sm, and ^{150}Sm exhibit a smooth variation, in accordance with the hydrodynamical model. The centroid energy of the GMR of ^{153}Sm is shown with dashed error bars in Fig. 6(a). Our value of $E_x = 15.3 \pm 0.14$ MeV for the GMR excitation energy in ^{144}Sm is somewhat higher but still in reasonable agreement with the values of 14.7 ± 0.2 and 14.6 ± 0.2 MeV found by the Grenoble[34] and Texas A&M (Ref. 35) groups, respectively. For ^{150}Sm there is excellent agreement between our value of 14.97 ± 0.18 MeV and the Grenoble datum[34] of 15.1 ± 0.25 MeV. However, our value of 15.52 ± 0.18 MeV for ^{152}Sm is considerably higher than the value of 14.8 ± 0.2 MeV obtained by the Grenoble group.[34] The reason for this discrepancy is not clear but might well be associated with the problem of continuum subtraction in both experiments. Anyhow, since ^{152}Sm is deformed, its GMR datum was not included in our data set used to determine the compressibility. In a deformed nucleus like ^{152}Sm the GMR will split into two components, as has been observed previously[34,35] for rare-earth nuclei. The energy and width of ^{152}Sm as shown in Fig. 6 refer to only the high energy component of the $E0$ strength. This component is shifted to higher excitation energy by ~ 0.6 MeV compared to its spherical neighbors. Abgrall *et al.*[38] predict on basis of a cranking model approach, a shift of $E_x = 5A^{-1/3}$ MeV for a nucleus with $\beta = 0.3$, amounting to 0.9 MeV. The experimentally observed shift in our data is slightly smaller than the above estimate. The same has been found to be true in other experiments.[34–37]

The strengths of the GMR and the GQR for Sm nuclei as calculated in terms of the EWSR are shown in Tables II and III. The GMR in these nuclei exhausts about 100–120% of the EWSR with a possible exception of ^{152}Sm. This would be in conformity with the known splitting of the GMR due to deformation. The other spherical nuclei exhaust almost full EWSR for both the GMR and the GQR.

C. Nuclear compressibilities

As mentioned in Sec. I, in the liquid-drop model the GMR energy is related to K_A by Eq. (1). However, in the scaling model it has been shown by Treiner *et al.*[5] that for a Gaussian strength distribution with a width (Γ) one should define E_0' by

$$E_0'^2 = E_0^2 + 3(\Gamma/2.35)^2 , \tag{7}$$

where E_0' is now related to K_A by the relation

$$E_0' = \hbar[K_A/(m\langle r_0^2\rangle)]^{1/2} . \tag{8}$$

Since we employ the assumptions of the scaling model in the expansion of K_A, we use Eqs. (5), (7), and (8) to fit the experimental data. The value of $\langle r_0^2 \rangle$ needed to calculate K_A has been calculated using the charge distribution parameters quoted by Bernstein.[39] The coefficient K_C' in Eq. (5), which is given as[3]

$$K_C' = 3/5(e^2/r_c)(1-27R) , \tag{9}$$

is related to K_∞ by the relation

$$R = \frac{\rho_0^2}{K_\infty} \cdot \frac{d^3\epsilon}{d\rho^3} . \tag{10}$$

It has been shown by Krivine *et al.*[40] that relation (10) can be evaluated to give

$$R = 0.5 - 45/K_\infty . \tag{11}$$

The parameter K_c' has been evaluated using Eqs. (9)–(11). The nuclear-matter compressibility K_∞ and the associated coefficients K_s' and K_Σ' in Eq. (5) have been obtained by a three-parameter fit of the experimentally observed energy systematics employing Eqs. (7)–(11). The nuclei included in the fit are all Sn isotopes and two spherical Sm isotopes (^{144}Sm and ^{148}Sm) studied here. In these fits we have taken account of the fact that the relative (statistical) uncertainties of ± 70 keV in the centroid energies for the GMR for the Sn and Sm nuclei which were mea-

sured in the same experiment are smaller than the total uncertainties of ±140 keV which include statistical and systematic errors. This leads to a slightly better determination of K'_Σ with the uncertainty of K'_Σ decreased by ~15%. All these nuclei exhaust the full $E0$ EWSR and do not seem to show any anomalous behavior in the systematics.

The parameters K_∞, K'_s, and K'_Σ as obtained from the fits on different sets of nuclei are shown in Table IV. The first set (a) corresponds to the nuclei studied in the present work. Set (b) includes the datum[25] on ^{208}Pb besides Sn and Sm nuclei of set (a). It can be noticed from the results of set (b) that the inclusion of a very heavy closed-shell nucleus like ^{208}Pb does not alter the parameters obtained using only the present data. The accuracy in the nuclear-matter compressibility and the surface parameter can be improved by extending the range of A, i.e., by including the light nuclei. This is necessary because the variation in $A^{-1/3}$ in the range of masses considered in these sets is not large enough to resolve the volume and the surface terms with higher accuracy. Thus, by including light nuclei one should be able to improve the accuracy with which one can resolve the surface and the volume terms. The third set (c) includes in addition to the nuclei of set (b) the datum[12] for ^{24}Mg for which almost the full $E0$ strength has been located.[12] In this set, the range of the $A^{-1/3}$ variations is considerably increased over that of sets (a) and (b). The results of set (c) show a slight change in the values of the parameters though not outside the error bars. The uncertainties in the value of the nuclear-matter compressibility and the surface parameters are reduced considerably as is obvious from the argument given above. These values are essentially the same as quoted in Ref. 16.

The curvature term, $K_{\rm curv} A^{-2/3}$, is important for light nuclei as it contributes a significant fraction to the compressibility of light nuclei.[16] It has been pointed out in microscopic calculations[41] employing various Skyrme interactions that the higher order terms including the surface symmetry term which occur in the expansion of the liquid-drop energy,[42] are negligible except for the curvature term. The curvature coefficient $K_{\rm curv}$ has previously been calculated[5] to be ~300 MeV in the scaling model. Including the curvature term in Eq. (5), we have performed fits on the nuclei of set (c). The coefficient $K_{\rm curv}$ is varied between 250 and 400 MeV with the other three parameters being fitted. We observe that the reduced χ^2 of the fits has a minimum when $K_{\rm curv}$ is taken to be ~375 MeV. This value is slightly higher than the value of $K_{\rm curv}$ calculated as 275 MeV using interaction SIII, and comparable to 340 MeV using SkM in the scaling model.[5] A negative value of this term from our fits is ruled out as the reduced χ^2 value of the fit increases considerably by taking a curvature coefficient as −300 MeV. The results of the fit are shown in set (d). These results are much closer to those of sets (a) and (b) for which the curvature correction is very small. It is clear that the data on Sn and Sm nuclei fit nicely with those of ^{208}Pb and ^{24}Mg. Thus, including all important terms in Eq. (5) for the nuclei under consideration, we determine the nuclear-matter compressibility and the associated parameters:

$$K_\infty = (300 \pm 25)\ \text{MeV}\ ,$$
$$K'_s = (-750 \pm 86)\ \text{MeV}\ , \tag{12}$$
$$K'_\Sigma = (-320 \pm 180)\ \text{MeV}\ .$$

It should be noticed that the results of the fit [Eq. (12)] remain unaffected by the choice of the starting values of the fit, implying that the fit is obtained at a deep minimum of χ^2.

The value of nuclear-matter compressibility, according to our data, is higher than the "commonly accepted" value (210±30) MeV (Ref. 3). This conclusion is in agreement with the results quoted in Ref. 13, where by using a different set of data including that for ^{28}Si, a value of $K_\infty = 270 \pm 13$ MeV was obtained without a curvature term. Also in Ref. 8 a fit is reported to the data of 33 nuclei with $64 < A < 208$: the resulting value of about 270 MeV for the nuclear compressibility without curvature term is again in good agreement with our value if no curvature term is included. This data set included the data for ^{64,66}Zn for which only a small amount of the EWSR was found. Thus all analyses using relations 6 and 7–11 seem to agree with each other in the sense that without a curvature term the value of the compressibility is around 270 MeV. Including the curvature term has the effect of

TABLE IV. The nuclear-compressibility parameters derived from fits on the GMR energies on various nuclei. The sets (a), (b), and (c) correspond to the present data and subsequent inclusion of ^{208}Pb and ^{24}Mg, respectively. The numbers in parentheses denote the total number of nuclei included in the fit.

Set of nuclei	Parameters obtained from fits K_∞ (MeV)	K'_s (MeV)	K'_Σ (MeV)	χ^2/N
(a) Sn(5) + Sm(2) = (7)	293±37	−640±155	−341±152	0.074
(b) Sn(5) + Sm(2) + ^{208}Pb = (8)	295±48	−647±192	−340±181	0.067
(c) Sn(5) + Sm(2) + ^{208}Pb + ^{24}Mg = (9)	272±25	−546± 89	−295±176	0.277
(d) including curvature term on set (c) with $K_{\rm curv} \sim 375$ MeV	301±25	−754± 89	−323±174	0.104

increasing this value to about 300 MeV. The χ^2/N values shown in Table IV are very low, while the precision with which the asymmetry term is determined is still not very satisfactory. Both these quantities are very much dependent on the uncertainties of ±70 keV assigned to the relative values of the GMR excitation energies for the Sn and Sm isotopes. If one would, for instance, decrease this value to ±40 keV, the absolute values of the various K-coefficients would barely change but the χ^2/N value would increase to $\cong 0.7$ while the uncertainty in the asymmetry coefficient would decrease to ±100 keV. However, we feel that such a small value in the uncertainty of the excitation energy is not justified, especially in view of the well-known problems associated with continuum subtraction. The value of K_∞ from our experiment is roughly in agreement[16] with the analysis of the electron scattering data by Có and Speth[22] who support a value of K_∞ of approximately 300 MeV or higher. Incidentally, a value of K_∞ higher than 210 MeV comes from the work of Glendenning[43] on the relativistic mean-field calculations on neutron-stars. By setting a constraint on the observed neutron-star masses, Glendenning[43] obtains a value of K_∞ in the vicinity of 285 MeV. This is in good agreement with our results. In a more recent work[44] in which the realistic masses of neutron-stars have been used, a lower bound of $K_\infty = 335 \pm 65$ MeV has been found.

VIII. CONCLUSION

The analysis of our data on Sn and Sm nuclei, along with the data on ^{208}Pb and ^{24}Mg shows that the nuclear-matter compressibility is higher than the commonly accepted value. We determine this important parameter from our precision data to be 300±25 MeV. The surface coefficient contributing to the compressibility has been deduced with a high accuracy as −750±86 MeV. Also, with the help of this data on isotopic chains, the asymmetry parameter K'_Σ, which was crudely known, has been determined to be (−320±184) MeV.

ACKNOWLEDGMENTS

We wish to thank T. D. Poelhekken, H. J. Hofmann, and S. K. B. Hesmondhalgh for their help during the experiment. One of the authors (M.M.S.) thanks the members of the Kernfysisch Versneller Instituut for excellent hospitality during his stay in Groningen. He also thanks Professor J. de Boer for support at Sektion Physik, University of Munich, where this work has been summarized, and Professors M. Brack, W. Stocker, and J. M. Pearson for many stimulating discussions. This work has been performed as part of the research program of the Stichting voor Fundamenteel Onderzoek der Materie (FOM), The Netherlands, with financial support of the Nederlandse Organisatie voor Zuiver Wetenschappelijk Onderzoek (ZWO).

[1]W. D. Myers and W. J. Swiatecki, Ann. Phys. (N.Y.) **84**, 186 (1974).
[2]V. R. Pandharipande, Phys. Lett. **31B**, 635 (1970).
[3]J. P. Blaizot, Phys. Rep. **64**, 171 (1980).
[4]M. Brack and W. Stocker, Nucl. Phys. **A406**, 413 (1983).
[5]J. Treiner, H. Krivine, O. Bohigas, and J. Martorell, Nucl. Phys. **A371**, 253 (1982).
[6]E. Baron, J. Cooperstein, and S. Kahana, Phys. Rev. Lett. **55**, 126 (1985).
[7]D. H. Youngblood, P. Bogucki, J. D. Bronson, U. Garg, Y.-W. Lui, and C. M. Rosza, Phys. Rev. C **23**, 1997 (1981).
[8]M. Buenerd, in Proceedings of the International Syposium on Highly Excited States and Nuclear Structure, Orsay, France, 1983 [J. Phys. (Paris) Colloq. **45**, C4-115 (1984), and references therein].
[9]M. N. Harakeh, in *Lecture Notes, XVII Summer School on Nuclear Structure by Means of Nuclear Reactions, Mikolajki, Poland, 1985,* edited by Z. Wilhelmi, G. Szeflinska, and M. Kicinska-Habior (Harwood Academic, Chur, 1987), p. 463.
[10]A. van der Woude, Prog. Part. Nucl. Phys. **18**, 217 (1987).
[11]J. Speth and A. van der Woude, Rep. Prog. Phys. **44**, 719 (1981).
[12]H. J. Lu, S. Brandenburg, R. De Leo, M. N. Harakeh, T. D. Poelhekken, and A. van der Woude, Phys. Rev. C **33**, 1116 (1986).
[13]Y.-W. Lui, J. D. Bronson, D. H. Youngblood, Y. Toba, and U. Garg, Phys. Rev. C **31**, 1643 (1985).
[14]J. P. Blaizot, D. Gogny, and B. Grammaticos, Nucl. Phys. **A265**, 315 (1976).
[15]J. P. Blaizot and B. Grammaticos, Nucl. Phys. **A355**, 115 (1981).
[16]A. van der Woude, W. T. A. Borghols, S. Brandenburg, M. M. Sharma, and M. N. Harakeh, Phys. Rev. Lett. **58**, 2383 (1987).
[17]G. E. Brown and E. Osnes, Phys. Lett. **159B**, 223 (1985).
[18]W. H. Dickhoff, A. Faessler, H. Muther, and S. S. Wu, Nucl. Phys. **A405**, 534 (1983).
[19]A. D. Jackson, E. Krotschek, D. E. Meltzer, and R. A. Smith, Nucl. Phys. **A386**, 125 (1982).
[20]B. ter Haar and R. Malfliet, Phys. Rep. **149**, 207 (1987).
[21]T. L. Ainsworth, E. Baron, G. E. Brown, J. Cooperstein, and M. Prakash, Nucl. Phys. **A464**, 740 (1987).
[22]G. Có and J. Speth, Phys. Rev. Lett. **57**, 547 (1986).
[23]J. Bartel, G. Wenes, M. Waroquier, and J. Ryckebusch, Mod. Phys. Lett. **A1**, 509 (1986).
[24]J. M. Cavedon, B. Frois, D. Goutte, M. Huet, Ph. Leconte, X. H. Phan, S. K. Platchkov, C. N. Papanicolas, S. E. Williamson, W. Boeglin, I. Sick, and J. Heisenberg, Phys. Rev. Lett. **58**, 195 (1987).
[25]S. Brandenburg, Ph.D. thesis, University of Groningen, 1985; S. Brandenburg, W. T. A. Borghols, A. G. Drentje, L. P. Ekström, M. N. Harakeh, A. van der Woude, A. Håkanson, L. Nilsson, N. Olsson, M. Pignanelli, and R. De Leo, Nucl. Phys. **A466**, 29 (1987).
[26]A. G. Drentje, H. A. Enge, and S. B. Kowalski, Nucl. Instrum. Methods **122**, 485 (1974).
[27]J. C. Vermeulen, J. van der Plicht, A. G. Drentje, L. W. Put, and J. van Driel, Nucl. Instrum. Methods **180**, 93 (1981).
[28]M. Di Toro, M. Pisa, and G. Russo, Phys. Rev. C **34**, 2334 (1986).
[29]G. R. Satchler, Part. Nucl. **5**, 105 (1973).
[30]C. M. Rozsa, D. H. Youngblood, J. D. Bronson, Y.-W. Lui,

and U. Garg, Phys. Rev. C **21**, 1252 (1980).
[31]M. N. Harakeh, program BEL, Kernfysisch Versneller Instituut Report 77i, 1981 (unpublished).
[32]W. Bauhoff, Z. Phys. A **318**, 219 (1984); G. J. Wagner, P. Grabmayr, and H. R. Schmidt, Phys. Lett. **112B**, 447 (1982).
[33]K. E. G. Löbner, M. Vetter, and V. Hönig, Nucl. Data Tables **A7**, 495 (1970).
[34]M. Buenerd, D. Lebrun, P. Martin, P. de Saintignon, and G. Perrin, Phys. Rev. Lett. **45**, 1667 (1980).
[35]U. Garg, P. Bogucki, J. D. Bronson, Y.-W. Lui, C. M. Rozsa, and D. H. Youngblood, Phys. Rev. Lett. **45**, 1670 (1980).
[36]S. Brandenburg, R. De Leo, A. G. Drentje, M. N. Harakeh, H. Janszen, and A. van der Woude, Phys. Rev. Lett. **49**, 1687 (1982).
[37]R. De Leo, S. Brandenburg, A. G. Drentje, M. N. Harakeh, H. Janszen, and A. van der Woude, Nucl. Phys. **A441**, 591 (1985).
[38]Y. Abgrall, B. Morand, E. Caurier, and B. Grammaticos, Nucl. Phys. **A371**, 253 (1982).
[39]A. M. Bernstein, in *Advances in Nuclear Physics,* edited by M. Baranger and E. Vogt (Plenum, New York, 1969), Vol. 3, p. 325.
[40]H. Krivine, J. Treiner, and O. Bohigas, Nucl. Phys. **A336**, 155 (1980).
[41]M. Farine *et al.* (private communication).
[42]M. Brack, C. Guet, and H. B. Hakansson, Phys. Rev. **123**, 275 (1985).
[43]N. K. Glendenning, Z. Phys. A **326**, 57 (1987); Phys. Rev. Lett. **57**, 1120 (1986); Astrophys. J. **293**, 470 (1985).
[44]N. K. Glendenning (private communication).